Solar Physics
DOI: 10.1007/●●●●●-●●●-●●●-●●●●-●

Post-eruptive arcade formation in 25 January, 2007 CME/flare limb event: microwave observations with the RATAN-600 radio telescope

I.U. Grigorieva[1] · **V.N. Borovik**[1] · **M.A. Livshits**[2] · **V.E. Abramov-Maximov**[1] · **L.V. Opeikina**[3] · **V.M. Bogod**[4] · **A.N. Korzhavin**[4]

Abstract The CME/flare event occurred by the eastern limb on 25 January 2007. Seven successive multi-wave solar observations in the range of 1.8 cm – 5.0 cm were carried out at the RATAN-600 radio telescope from the very beginning of post-eruptive arcade formation (30 min after the C6.3 flare peak) and lasted for 3.5 hours. There were favourable conditions for studying the off-limb microwave radio source associated with the post-eruptive arcade in different phases of its formation. Microwave radio emission of the arcade was rather intensive at initial stage and considerably decreased at decay stage; its maximum was positioned on the 195 Å Fe XII loop tops. The RATAN-600 total flux spectra of the off-limb radio source were practically flat in the initial phase and showed the predominant contribution of thermal emission. Later, in the decay phase, the thermal contribution considerably decreased in the course of arcade development. Furthermore, observational data available in the meter wavelength range were indicative of non-thermal processes in arcade at least during three hours from the beginning of its formation. The obtained microwave data are interpreted as a thermal free-free emission of a large hot plasma cloud and a non-thermal contribution due to particle acceleration. This event supports the model in which the post-eruptive arcade is formed in a hot gas cloud which arises after CME and the impulsive phase and moves downward. Hot gas inside this cloud is affected by the plasma flow and accelerated particles originated from the coronal current sheet (reconnection region).

Keywords: Coronal Mass Ejections, Initiation and Propagation; Flares, Energetic Particles

[1] Central Astronomical Observatory at Pulkovo,Russian Acad. Sci. email: borovik@mk4099.spb.edu
[2] Pushkov Institute of Terrestrial Magnetism, Ionosphere and Radiowave Propagation of Russian Acad. Sci.
[3] Special Astrophysical Observatory of Russian Acad. Sci.
[4] Saint-Petersburgs Branch of SAO RAS

1. Introduction

Consideration of coronal mass ejection (CME) and the related flare as two parts of the same event is the basic tendency in developing of our knowledge about non-stationary solar phenomena. The main features of a solar eruptive event are determined by the magnetic configuration and velocity field. The relation between ejection (jet or CME) and the flare itself is rather complicated and now it is being widely studied (see the Topical Issue on "Radio Physics and the Flare-CME relationship" (Solar Phys., in press) and (e.g. Shakhovskaya, Livshits, and Chertok, 2006).

In the course of most of rather major flare/CME events a part of magnetic field lines is blown open after the eruption. Later some open lines are transformed again into a closed configuration by reconnection process with the current sheet formation. Then, the loops located under the formed current sheet shrink, but plasma above the current sheet is thrown out into the interplanetary space. The ascending loop system observed after powerful eruptive events is the result of the magnetic field reconnection in the corona. These considerations are a part of the current sheet scenario known as "CSHKP" ("standart") flare model (Carmichael, 1964; Sturrock, 1966; Hirayama, 1974; Kopp and Pneuman, 1976).

In this paper, the CME/flare event occurred by the E-limb on 25 January 2007 is considered. Here we concentrate on the formation of post-eruptive arcade. Formerly post-flare loops were observed in H_α line and in SXR (Yohkoh). Now, when dynamic flares occur, they are well detected by SOHO/EIT and TRACE in 195 Å FeXII and in other ranges.

Long living microwave radio sources (some of them being off-limb at a height up to 170000 km) were reported about two decades ago (e.g. Borovik *et al.*, Urpo *et al.*, 1989, 1989). These sources were related to post-flare manifestations, but, because no regular soft X-ray observations were available at that time, they could not be directly identified with post-eruptive arcades. In the last years those long-lived coronal formations were studied using multi-spectral data and radio astronomy methods. New important information on plasma parameters in the post-eruptive arcades was obtained by the telescope SPIRIT on board CORONAS-F (Zhitnik *et al.*, 2003), especially in Mg XII 8.42 Å.

The results of complex studies of post-eruptive arcades in eruptive phenomena of 2 November 1992, 22 October 2001, 12 November 2001 and 28–29 December 2001 in which we took part are briefly summarized here. First of all, we note that in these events the post-eruptive arcades were observed after one or more CMEs. The related flares had different power and belonged to different X-ray classes, namely: 2 November 1992 – class X9, 28 December 2001 – X4.0, 22 October 2001 – M1.0, and 12 November 2001 – C7.0.

In events mentioned above the observations of arcades were made at the late post-eruptive stage, 6–12 hours after the peak of the related flare. Plasma parameters in the post eruptive arcades turned out to be the following: the temperature in the sources of microwave and SXR emission was 5–10 MK and the electron density was $(5-10)\times10^9 cm^{-3}$ in the decay phase. The observational results indicated a prolonged energy release high in the corona manifesting itself both in long-lasting heating capable to maintain a high temperature in the arcade

for a long time with a much higher temperature of its top part and in detectable non-thermal processes even at late post-eruptive stage (Grechnev *et al.*, 2006a, 2006b; Borovik *et al.*, 2007).

The observations at the initial stage of the post-eruptive arcade formation, just after the flare peak, are crucial for understanding the origin of formation of long living high loop structures. We succeeded in such observations of CME/flare limb event of 25 January 2007 with the RATAN-600 radio telescope. The results of observations with the analysis of this non-stationary phenomenon are given in this paper. Section 2 describes observations carried out at the RATAN-600 radio telescope. Section 3 is devoted to the features of CME/flare limb event and the related phenomena in different ranges with the analysis of RATAN-600 data. The discussion and some conclusions are given in Section 4.

2. RATAN-600 data

In January 2007 solar observations were carried out daily at the RATAN-600 radio telescope in the celestial meridian and six azimuths (one observation was at local noon , three – before noon and three – after noon) with time-intervals of about 35 min. Right and left circularly polarized components (RCP and LCP) were recorded at 44 wavelengths simultaneously in the wavelength range of 1.8 – 5.0 cm during the Sun crossing the fixed diagram of antenna. The total intensity (Stokes parameter "I") and the circularly polarized component (Stokes parameter "V") are calculated as $I = RCP + LCP$ and $V = RCP - LCP$. The beam width (HPBW) is $17'' \times 13'$ at 2.0 cm.

On January 25, the solar observations were made at 07:44, 08:18, 08:52, 9:26 (local noon), 10:00, 10:34 and 11:08 UT from the very beginning of the post-eruptive arcade formation (30 min after the flare peak) and lasted 3.5 hours. The moments of RATAN-600 observations are shown in Figure 1 by vertical lines. Microwave radio emission of the related active region NOAA 10940 situated behind the E-limb on January 25 was recorded only the next day. This circumstance provided favourable conditions for study microwave radio emission of the post-eruptive arcade.

Figure 2 (*panel* a) shows, as an example, a one-dimensional RATAN-600 solar scan (Stokes "I") at 3.0 cm overlaid on SOHO/EIT 195 Å Fe XII image (negative). The orientation of the solar image was changed to fit the RATAN-600 observations. In the scan one can see an off-limb (E) radio source associated with the post-eruptive arcade and another one by the W-limb associated with the active region NOAA 10939. The error of co-alignment of the scan and 195 Å solar image is assumed to be 5 arc sec. We used the radio sources (in "I" and "V" channels) associated with bright points in 195 Å solar image and the leader sunspot of the NOAA 10939 to control co-alignment.

In Figure 2 (*panel* b) a part of the solar scan by E-limb obtained at the shortest wavelength of the operative range 1.84 cm ("I" and "V") at 09:26 is given. One can see two components of the off-limb radio source (shown by arrows) which are resolved due to higher spatial resolution of antenna at this wavelength.

The RATAN-600 data have two major advantages: very high sensitivity due to the huge effective area of the antenna system, and multi-frequency observations

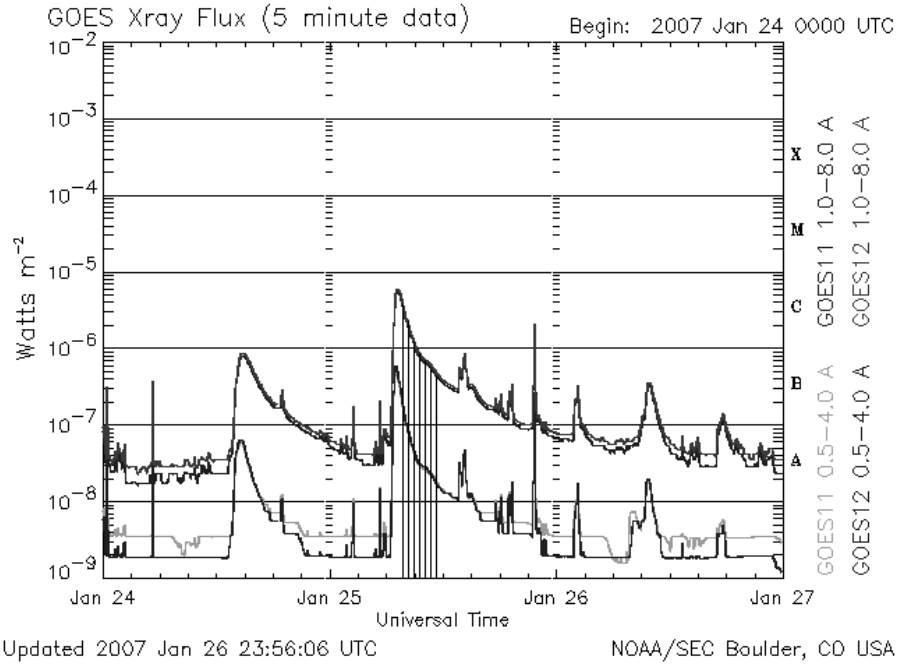

Figure 1. GOES X-ray plot of 5 minute averages of solar X-ray output in the 0.1–0.8 nm and 0.05–0.4 nm passbands for the 24–26 January 2007. Vertical lines show the moments of RATAN-600 observations.

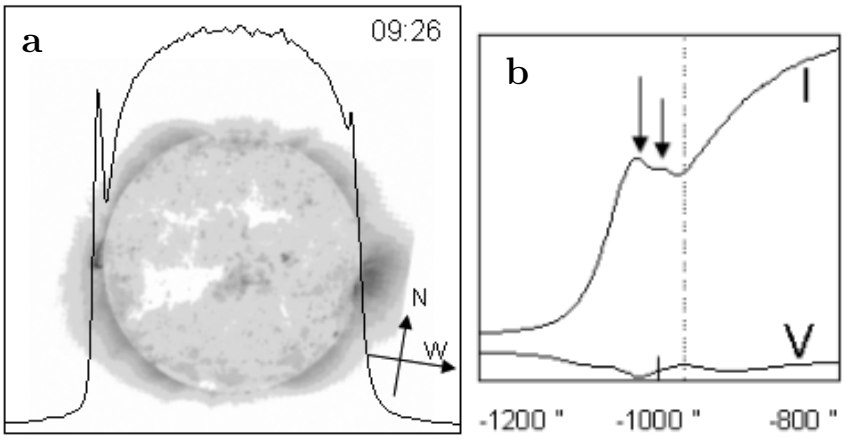

Figure 2. a) One-dimensional RATAN-600 solar scan (Stokes "I") at 3 cm at 9:26 UT overlaid on the SOHO/EIT 195 Å Fe XII image at 9:24 UT (negative). The cross with arrows in the right bottom corner shows N-S and E-W directions on the solar disk. b) East-part of the solar scans at the wavelength 1.8 cm ("I" and "V") at 09:26 UT. Arrows show two components of the off-limb radio source. Dashed line shows the solar limb.

in a wide microwave range. At the same time, there are two disadvantages – the ambiguity of the one-dimensional data and the instrumental polarization contribution at the solar limb due to specific antenna configuration. To extract reliably the off-limb source in solar scans obtained on January 25, we used the scans of the previous day (January 24), when neither by-limb, nor off-limb radio sources were present.

In Figure 3 one can see a sequence of off-limb radio sources extracted in the scans at 2.4 cm in channel "I" (*panels* a–f) and in channels "I" and "V" (*panel* g) overlaid on post-eruptive arcades negative images (195 Å SOHO/EIT). Solid lines under the radio sources show the direction of the Sun scanning in the RATAN-600 observations.

The evolution of the post-eruptive arcade in 195 Å is seen in Figure 3 as well as in Figure 4. The orientation of the solar image (positive) in Figure 4 was changed to fit RATAN-600 observations. Here the vertical solid lines show the locations of peak intensity of the off-limb radio source and the dotted vertical lines show the location of the second component of the radio source (when it could be resolved). The available images of the arcade (195 Å SOHO/EIT) are given at the moments which are nearest to those of the RATAN-600 observations. In *panels* (a,b) one can see a bright diffuse source close to the E-limb (at 07:36 and 07:48). The first loop system (labeled by "1") is seen in the next RATAN observation at 08:18 (*panel* c). According to 195 Å images (*panels* c–h) the height in plane-of-sky of the largest loop "1" changed from 25000 km at 08:12 to 35000 km at 09:24 and to 50000 km at 11:12. The apparent ascending velocity of loop "1" in this time interval was practically constant 2.3 kms^{-1}. The 195 Å images obtained by SOHO/EIT after 11:12 show that ascending velocity of this loop slowed down. It is in accordance with the evolution of H_α and SXR post-flare loops in the well studied limb event of 2 November 1992 (Kamio, Kurokawa, and Ishi, 2003). Another loop system (labeled by "2" and "3") appeared northward and developed as the time went on (see *panels* d–h). One can see in Figure 4 that in all the RATAN-600 observations the maxima of intensity of the microwave emission (solid vertical lines) are positioned on the tops of 195 Å arcades. From the latest RATAN-600 observations it is seen that the locations of a second component of the off-limb radio source, when it is resolved, (shown by dotted lines) coincide with the upper part of a new "northern" loop system (labeled by "2" and"3"in *panels* d-h).

It should be noted that it is difficult to estimate reliably the intensity and effective sizes of the two components of the radio source. However, it can be concluded from the two latest RATAN-600 observations that the microwave emission of the northern (new) loop system ("3") is more intensive than that of the southern (old) one ("1"). At the same time, the radio emission of the "old" loop system is more polarized (degree of circular polarization is about 15%) than that of the "new" one. Figure 3 (*panel* g) confirms this fact.

Here we concentrate on the total characteristics of the off-limb microwave radio source associated with the whole post-eruptive arcade and their evolution in the course of arcade formation. Taking into account the beam width (FWHM) of the RATAN-600 radio telescope in the operating wavelength range (1.84 cm – 5.02 cm), we estimated the effective size "D" of the microwave emitting region.

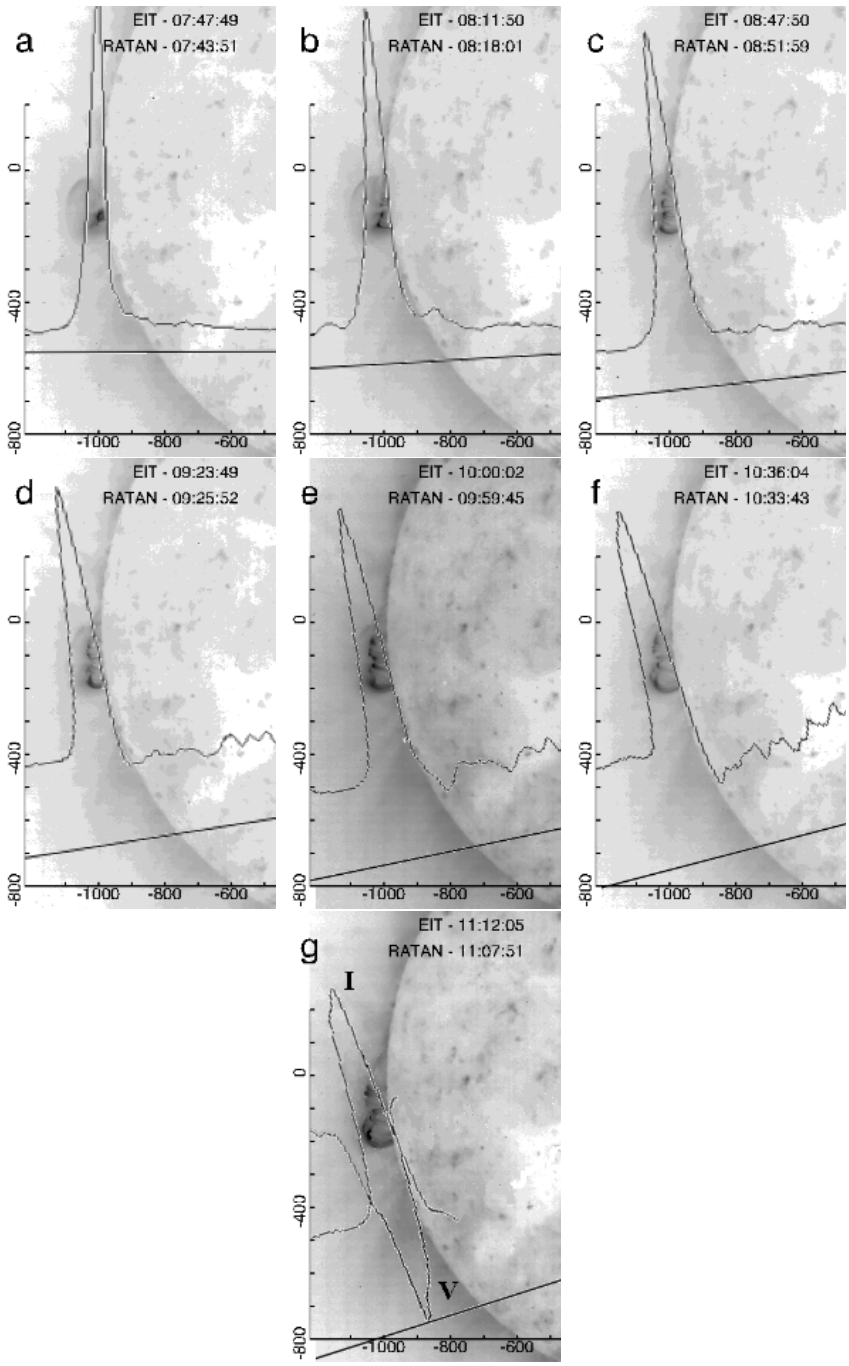

Figure 3. Sequence of the off-limb radio sources extracted in the RATAN-600 scans at 2.4 cm in channel "I" (*panels* a–f) and in channels "I" and "V" (*panel* g) overlaid on the post-eruptive arcade negative images (195 Å SOHO/EIT). Solid lines under the radio sources show the direction of Sun scanning in RATAN-600 observations. Axes show arc seconds from the solar disk center.

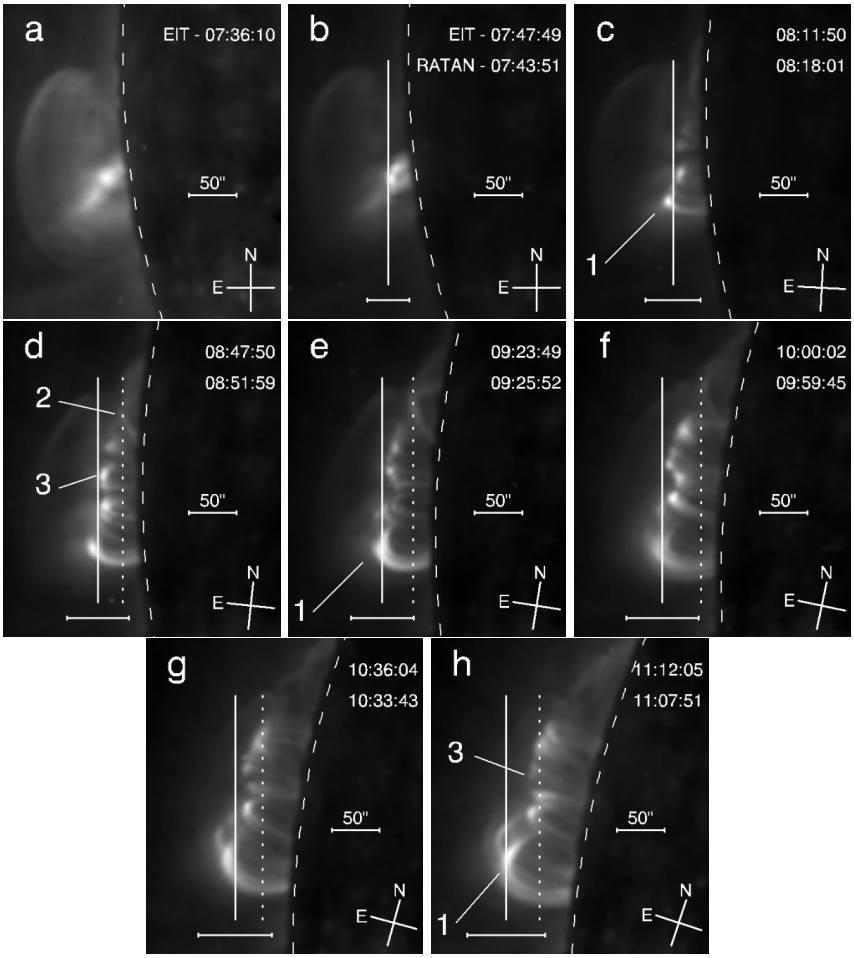

Figure 4. Sequence of 195 Å images of post-eruptive arcade on 25 January 2007 obtained at the moments near RATAN-600 observation moments. Solar images are rotated so that the Sun scanning direction on RATAN-600 is horizontal. Vertical solid lines show the locations of peak intensity of the off-limb radio source and the dotted vertical lines show the location of the second component of the radio source (where it could be resolved). Solar optical limb is shown by dashed line. Horizontal segments under the arcades show effective sizes of the off-limb radio sources. The crosses in the right bottom corners show N-S and E-W directions on the solar disk. The meaning of digits "1", "2" and "3" see in the text.

It is given in Table 1 for different times of the RATAN-600 observations. The sizes are shown in *panels* (b–h) by horizontal segments under the arcade. In the first observation the effective size of the microwave emitting region is larger than that of small loop in 195 Å by the limb. In the later observations the radio sizes are found to be approximately the same as the projections of the whole loop system on the direction of scanning.

The evolution of total flux spectra of the off-limb radio source associated with the post-eruptive arcade can be seen in Figure 5. The spectra are constructed as the upper envelope of spectra obtained by using all wavelengths in

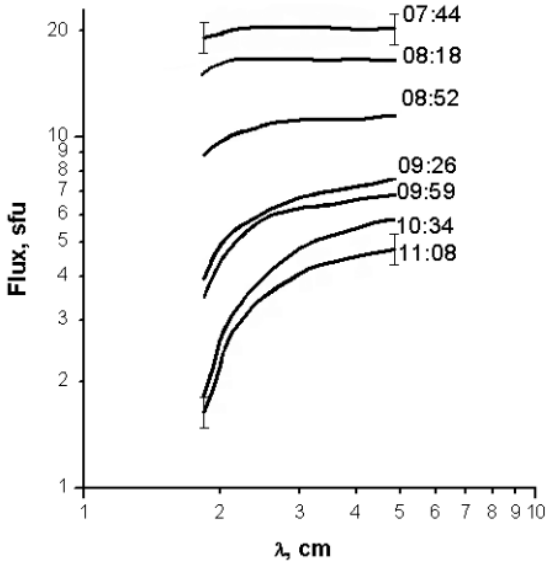

Figure 5. Averaged total flux microwave spectra of the off-limb radio source associated with post-eruptive arcade at different moments of RATAN-600 observations.

the operating range. The error in flux measurements (10%) is determined by the accuracy of both the separation of the off-limb source and the calibration technique. For absolute calibration we used the Moon and Crab Nebula observations made with the RATAN-600 radio telescope. The total fluxes of solar radio emission in microwaves measured at different solar stations (Nobeyama, Pentincton, Learmonth) were also taken into account.

We estimated the effective brightness temperature of the off-limb radio source at 5 cm using expression

$$T_b(K) = 5.45 \cdot 10^3 S \lambda^2 D^{-2},$$

where is S a flux density (sfu), λ - wavelength (cm), D - effective size of the radio source (arc min). The values of S and T_b obtained at different times of the RATAN-600 observations are given in Table 1. Adopting the thermal bremsstrahlung of the optically thin plasma at the shortest wavelength with temperature $T = 5$ MK at the time of the first RATAN-600 observation (07:44) from a well-known expression

$$S(sfu) \sim 3 \cdot 10^{-45} EM(cm^{-3}) T(K)^{-1/2}$$

we get the column emission measure $EM = 1.5 \cdot 10^{49} cm^{-3}$ and the electron density in the emitting region as $N_e = \sqrt{(EM/V)} = 2.3 \cdot 10^{10} cm^{-3}$ (assuming that the volume of the arcade $V = D^3$, where D is a effective size of the radio source associated with the arcade at 07:44).

Table 1. Radio flux density S, effective size of the radio source D and effective brightness temperature T_b of the off-limb radio source at 5 cm.

Time, UT	S (flux density), sfu	D, arcsec	T_b,MK
07:43:51	20.5	44	5.3
08:18:01	16.5	58	2.4
08:51:59	11.6	64	1.5
09:25:52	7.7	66	0.87
09:59:45	6.8	77	0.56
10:33:43	5.9	76	0.5
11:07:51	4.8	82	0.35

3. Analysis

The limb event on 25 January 2007 consisted of a CME and related 6.3 class flare (S08E90). In GOES data, the flare onset was 06:33 and peak emission occurred 07:14. The event began to develop against the faint post-eruptive loops associated with the previous event – CME and B9.0 class flare which occurred behind the eastern limb on 24 January 2007 between 13:45 – 16:00.

According to SOHO/LASCO data of January 25, a strong wave signature could be seen propagating toward the front side by 06:48. By 08:30 faint and diffuse extensions surrounded the C2 occulting disk. The event was seen in C3 at 07:42, all above the E limb with shock signatures to N and S, which seemed to surround the C3 occulting disk by 08:42. By 09:42, the C3 occulting disk appeared surrounded and from there on the event looked as a whole as a very asymmetric halo. The mean plane-of-sky speed of the event at PA $\sim 90^\circ$ was 1260 kms^{-1} showing a decelerated profile.

The northern part of the CME-loop was brighter than the southern one (see Figure 6). The main feature of these CME was a very large expanding bright front which occupied the most part of the eastern limb. According to 3/LASCO data, the front of disturbance was not effectively pronounced. This was consistent with a weak driven-shock which went far towards the corona. The mass of CME was somewhat less than 10^{16} g, which is typical of a powerful CME/flare events.

Many manifestations of the expanding coronal "wave" along the Sun's surface have been detected in this event (Attrill *et al.*, 2007). Flare generated Moreton waves sometimes activate filaments located far from the flare site. A recent example of such an activation occurred on 6 December 2006 in which a large flare occurring near the east limb caused a dynamic response in a filament located far to the south (Gilbert, de Toma, and Tripathi, 2007).

The RHESSI observations were made at time intervals of 06:33–07:10 and 07:45–08:45. In Figure 7 one can see that the flux of low-energy (3–25 keV) photons was increasing rather slowly during the impulsive phase of the related flare and reached a comparatively small value. The reliable signal in the 3–6 keV and 6–12 keV channels was registered the flux progressive decreasing during the

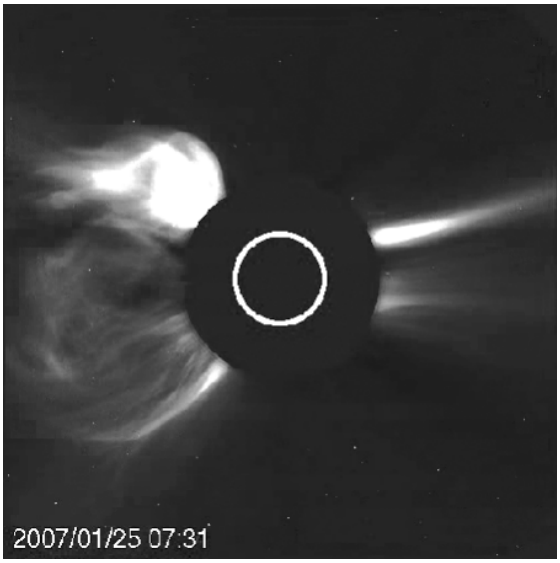

Figure 6. CME image by SOHO/LASCO/C2 at 07:31 UT on 25 January 2007

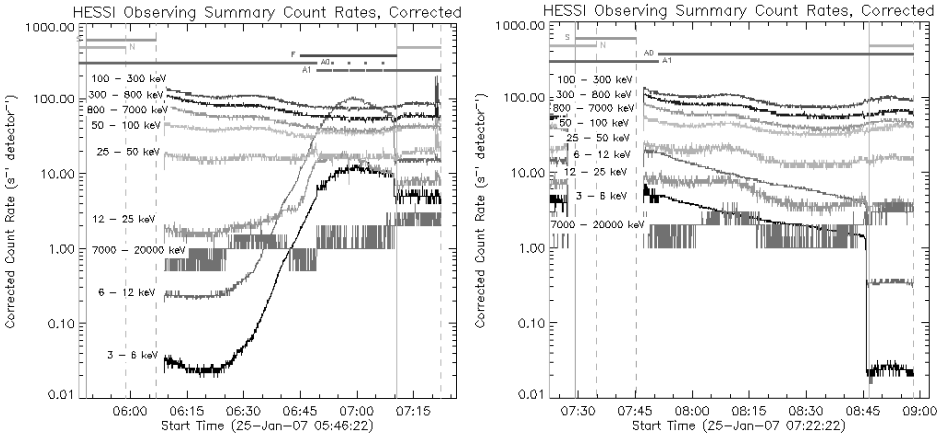

Figure 7. RHESSI observing count rates (25 January 2007). In left panel (from bottom to top: 3–5 keV, 6–12 keV, 7000–20000 keV, 12–25 keV, 25–50 keV, 50–100 keV, 800–7000 keV, 300–800 keV and 100–300 keV; in right panel (from bottom to top): 7000–20000 keV, 3–5 keV, 12–25 keV, 6–12 keV, 25–50 keV, 50–100 keV, 800–7000 keV, 300–800 keV and 100–300 keV.

second observational interval. No high-energy photons have been registered by RHESSI.

According to RHESSI reconstructed images in the 12–25 keV channel the sources located just above the arcade in 195 Å images were registered at 07:51, 09:21 and 10:51.

The characteristic feature of the related C6.3 flare was a rather slow increase of emission (in GOES and RHESSI ranges) and a slow emission decrease after the peak. It is not typical of most of the flares of such power. Probably, it is due

to the fact, that the lower parts of some loops were situated behind the solar limb. As it is seen in 195 Å arcade images a new (northern) system of loops began to develop after the southern one. That might be the reason for a reduced rate of the SXR-emission decrease after the peak. It would be possible to connect a rather low X-lass of the flare with the fact that the northern foot points of the flare loop were located behind the limb and their SXR-emission did not reached the observer.

In the radio range the impulsive phase of this weak flare was well detected at the wavelengths longer than 6 cm up to meter wavelengths (204 Hz). It is seen in Figure 8 where multi-channel time profiles of radio fluxes (LEARMONTH and IZMIRAN data) are given.

According to the open data of radio-spectrographs at LEARMONTH station and IZMIRAN, a large group of type III bursts were detected at 06:43–06:54 followed by the low frequency ($<$ 50 MHz) slowly drifting type II burst at 06:45–06:50. This weak type II radio burst was registered apparently in WIND observations in the frequency range of 0.09–14 MHz. The frequency of the peak of this burst decreased from 10 to 3 MHz during 12 min.

The continuum (noise storm) with many bursts with duration of about some seconds appeared simultaneously with the impulse phase at frequencies $<$ 120 MHz. From 07:15 this continuum extended to the high-frequency range 115–170 MHz, and was observed in this range to 07:50. Then both low and high frequencies of continuum began to drift toward low frequencies. In the range $<$ 100 MHz these phenomena were observed at the whole time (07:15–10:30), with more intensive manifestation at about 08:00.

Summarizing all the facts described above one can conclude that the CME-flare-event studied in this paper was rather weak. It is characterized by both a rather slow increase and slow decrease of SXR-emission. At the same time it is similar to the usual LDE event, which is characterized by large-scale processes. Indeed, the CME occupied nearly the whole eastern limb. As it was mentioned above, there were many manifestations of the expanding coronal "wave" along the Sun surface.

The impulse was weak, and the post-eruptive arcade formation does not correspond to GOES class of the related flare. The absence of hard ($>$ 50 keV) X-ray emission and, consequently, the absence of corresponding high-energy particles accelerated during the impulsive phase provided favourable conditions for microwave observations of the arcade formation.

We compare the RATAN-600 microwave data with some features of this event which were manifested in meter radio range.

The RATAN-600 microwave observations continued for 3.5 hours with the time resolution of 35 min. The time interval of RATAN-600 observations coincides with the process of the post-eruptive arcade formation including its initial stage, and obtained data reflect this process. Two fist RATAN- 600 observations were made at the initial stage of post-eruptive arcade development (at 07:44 and 08:18). Just at that time (07:45) the second peak of emission after the impulsive phase was recorded at 245 MHz (LEARMONTH) as well as at 204 and 169 MHz (IZMIRAN). This peak in details can be seen in Figure 8(c). Here a fragment of the time profile (10 sec averaging) at frequency 245 MHz (LEARMONTH)

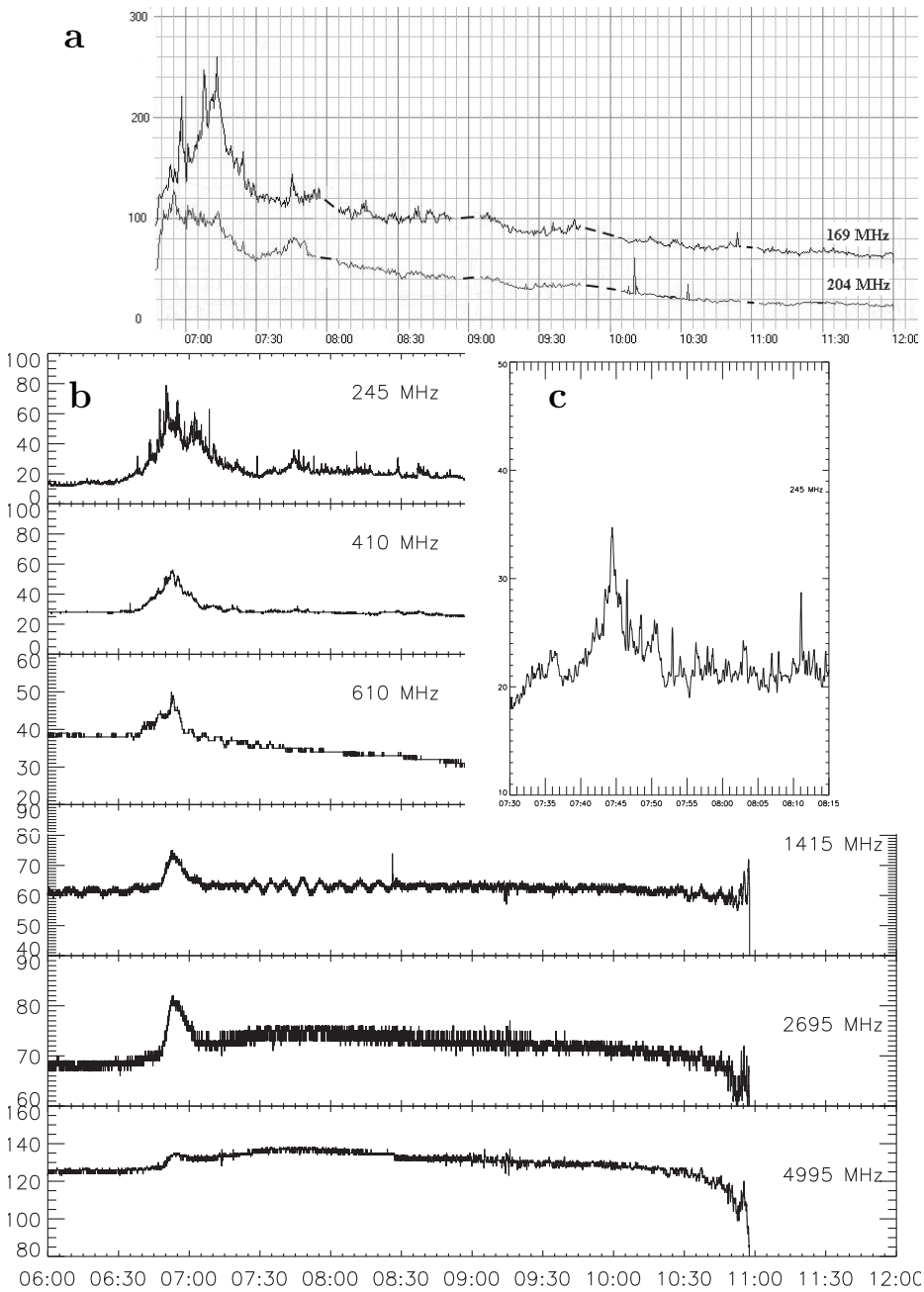

Figure 8. Multi-channel time profiles of radio emission: a – IZMIRAN data; b – LEARMONTH data; c – fragment of LEARMONTH time profile at 245 MHz (with 10 sec averaging) for time interval 07:30 – 08:15

for the time-interval 07:30–08:15 is given. It might be supposed that this second peak is due to the presence of hot plasma and fast particles in the observed region at this time.

The arcade 195 Å images (SOHO/EIT) given in Figure 4 (*panels* a–b) show a bright diffuse formation close to the E-limb at 07:36–07:48. Later, as the flare proceeds, the set of loops ascending above the solar limb during several hours are well seen. At first, the southern part of the arcade appeared and then the northern one. The RATAN-600 data showed that the microwave emitting region was co-spatial with the top of the loop structure during the whole period of observations. One can suppose that in the first two RATAN-600 observations we see the transformation of the diffuse hot plasma cloud into a structured formation. The appearance of the second maximum in the meter radio emission at this time interval (07:45) is likely to indicate the role of fast electrons in the arcade formation process.

The RATAN-600 microwave total flux spectra (see Figure 5) show a great contribution of thermal emission, especially at the initial stage of the arcade formation. Later, as the arcade developed, the thermal contribution considerably decreased. At the same time the radio data at meter wavelengths presented above are indicative of non-thermal processes up to 10:30. The microwave spectra (RATAN-600) confirm that the radio emission during the whole period under consideration was generated both by thermal and non-thermal mechanisms.

4. Discussion

The CME/flare event occurred behind the eastern limb on 25 January 2007. Seven successive multi-wave solar observations in the range of 1.8 cm – 5.0 cm were carried out at the RATAN-600 radio telescope from the very beginning of post-eruptive arcade formation and lasted 3.5 hours. The related C6.3 class flare was registered against a low X-ray background. The associated active region NOAA 10940 was situated behind E-limb, and its microwave radio emission was recorded only the next day. These circumstances provided very favourable conditions for studying the off-limb microwave radio source associated with the post-eruptive arcade at different stages of its development.

The RATAN-600 data showed that the microwave radio emission of the arcade was rather intensive at initial stage of its formation and considerably decreased during its later developing and rising above the limb. The maximum microwave emission of the off-limb radio source associated with the arcade was positioned on the 195 Å Fe XII loop tops at all stages of arcade expansion. The total flux spectra of the off-limb radio source were practically flat in the range of 2–5 cm at the initial stage (30 min – 1 hour after the peak of the flare) and showed the predominant contribution of thermal emission. Later, in the decay phase, the thermal contribution considerably decreased in the course of the arcade development. Moreover, the observational data available in the meter wavelength range were indicative of the non-thermal processes in the arcade at least for three hours from the beginning of its formation. The obtained radio data may be interpreted as thermal free-free emission of a large hot plasma cloud, and a

non-thermal contribution due to the accelerated particles. This result confirmed our previous conclusions in post-eruptive arcade investigations (Grechnev *et al.*, 2006a, 2006b; Borovik *et al.*, 2007) and added some new information on the initial stage of the post-eruptive arcade formation.

One of the goals of this work was to check the conception of the origin of the post-eruptive arcade formation, which has been reported at the Workshop "X-ray Spectroscopy and Plasma Diagnostics from the RESIK, RHESSI and SPIRIT instruments" in Wroclaw, in December 2005 and is to be published (Livshits, 2007). This conception based on results by Sheeley, Warren, and Wang, 2004, supposes that the bulk of plasma is thrown out first into corona and then into the interplanetary space as the CME/flare occurs. However, a part of plasma falls down. The magnetic reconnection is likely to be going on in the vertical current sheet in the decay phase of the eruptive event. As a result, the current sheet causes the moving downward flow of hot plasma and accelerated particles, which reinforced the falling matter. At the same time, the accelerated particles and plasma thrown out into the high corona cause the sources of radio emission in meter wavelength range in the corona.

The appearance of a hot plasma cloud after flare impulsive phase and CME might be supposed. In this cloud the post-eruptive loops begin to form due to the matter falling onto the magnetic field lines (horizontal dipole). Later, even not very high heating of the plasma in the loop tops may provide an expansion and a very long existence of those loops for several hours

This conception was motivated by the observational data obtained by TRACE in 195 Å and RHESSI (3–100 keV) in the event of 21 April 2002 (X1.5 class flare) (Gallagher *et al.*, 2002). The TRACE movie showed directly the flows of hot plasma moving downward which were later studied by Sheeley, Warren, and Wang, 2004. Note, that there are several common features in the events of 21 April 2002 and 25 January 2007. Namely: the hot plasma cloud formation and appearance of post-eruptive loops one hour after the flare peak; the development of a secondary loop system. Radio emission in the meter wavelength range was detected in both events. However, the flare on 21 April 2002 was more powerful and it occurred by the western limb and not by the eastern one as it was on 25 January 2007. As a result, there were better conditions in the event of 21 April 2002 for detecting accelerated particles and fine radio structure at meter wavelengths, which were recorded with the spectrometer of National Astronomical Observatory of China (NAOC) and studied in details (Chernov *et al.*, 2005). Moreover, the impulsive phase of the flare in the event of 21 April 2002 was manifested more obviously by the source of hard X-ray emission above the post-eruptive loops, probably, in the site of the current sheet. At the same time, many accelerated particles might cause difficulties in detecting a thermal component of radio emission during the arcade formation.

In the case of 25 January 2007 the observations of arcade formation was carried out beyond the solar disk and beyond the active region. It provided better conditions for detecting the ending of the weak impulse and appearance of the loops. After the impulse phase a current sheet formed and began to rise higher and higher. But it was not very strong as it follows from the absence of the X-ray emission in the range > 50 keV.

One can conclude that the results obtained in this study are import for solving some urgent problems of investigating CME/flare events. The most important of them is the relation between CME, the proper flare and the arcade formation. Physical conditions in the region of its formation may be determined by the X-ray data (RHESSI), by CORONAS-F data (particularly in line Mg XII) and by TRACE movies. The microwave radio off-limb observations provide additional information on the arcade formation. In our case the RATAN-600 observations allowed us to trace the evolution of the hot plasma cloud during some hours after the flare. The fluxes of microwave emission at short wavelengths show fast decrease of the emission measure of the thermal source. Apart from that the comparison of the RATAN-600 data with the observations at meter wave lengths allows us to believe that the region of the main microwave emission was rising gradually higher and higher following the source of the accelerated particles which are likely to have been generated in the moving upward current sheet.

The more detailed comparison of the results of this paper with some model conceptions as well as determination of the characteristics of the accelerated particles and their source are beyond the frame of this paper and will be considered later on.

Acknowledgements We are grateful to V.V. Grechnev, G.P. Chernov and I.M. Chertok for fruitful discussion. We thank the instrumental teams of the RATAN-600 radio telescope, IZMIRAN and LEARMONTH stations and SOHO, GOES, RHESSI missions for the open-data policies which made available for us data used in this study. SOHO is a project of international cooperation between ESA and NASA. This work was supported by the Russian Foundation for Basic Research under Grants 05–02–17105, 06–02–16838, 06–02–17357, 06–07–89002 and by Presidium of Russian Academy of Sciences under a grant OFN-16. B.V.N. thanks LOC "CESRA-2007" for financial support.

References

Attrill, G.D.R., Harra, L.K., van Driel-Gesztelyi, L., Demoulin, P., Wulster, J.-P.: 2007, *Astron. Nachr.* **328** (8), 760.

Borovik, V.N., Gelfreikh, G.B., Bogod, V.M., Korzhavin, A.N., Krüger, A.: 1989, *Solar Phys.* **124**, 157.

Borovik, V.N., Grechnev, V.V., Abramov-Maximov, V.E., Grigorieva, I.Y., Bogod, V.M., Kaltman, T.I., Korzhavin, A.N.: 2007, in Zaitsev, V.V.,Bogod, V.M.,Stepanov, A.V. (eds.), *Proceedings of Conference on Multiwaves Researches of the Sun, SAO, September 28 - October 2, 2006*, S.-Petersburg, 370 (in Russian).

Carmichael, H.: 1964, in W.N.Hess (ed.), *AAS-NASA Symp on the Physics of Solar Flares*, Washington , D.C.: NASA, 451.

Chernov, G.P., Yan, Y.H., Fu, Q.J., Tan, Ch.M.: 2005, *Astron. Astrophys.* **437**, 1047.

Gallagher, P.T., Dennis, B.R., Krucker, S., Schwartz, R.A., Tolbert, K.: 2002, *Solar Phys.* **210**, 341.

Gilbert, H., de Toma, G., Tripathi, D.: 2007, American Astronomical Society Meeting 210, No 25.05.

Grechnev, V.V., Kuzin, S.V., Urnov, A.M., Zhitnik, I.A., Uralov, A.M., Bogachev, S.A.,. Livshits, M.A., Bugaenko, O.I., Zandanov, V.G., Ignat'ev, A.P., Krutov, V.V., Oparin, S.N., Pertsov, A.A., Slemzin, V.A., Chertok, I.M., Stepanov, A.I.: 2006, *Solar System Research* **40**, (4), 286.

Grechnev, V.V., Uralov, A.M., Zandanov, V.G., Rudenko, G.V., Borovik, V.N., Grigorieva, I.Y., Slemzin, V.A., Bogachev, S.A., Kuzin, S.V, Zhitnik, I.A., Pertsov, A.A., Shibasaki, K., Livshits, M.A: 2006, *Pub. Astron. Soc. Japan* **58**(1), 55.
Hirayama, T.: 1974, *Solar Phys.* **34**, 323.
Kamio, S., Kurokawa, H., Ishi, T.T.: 2003, *Solar Phys.* **215**, 127.
Kopp, R.A. and Pneuman, G.W.: 1976, *Solar Phys.* **50**, 85.
Livshits, M.A.: 2008, *Astronomy Reports* **52**, in press.
Shakhovskaya, A.N., Livshits, M.A., Chertok, I.M.: 2006, *Astronomy Reports*, **50** (12), 1013.
Sheeley, N.R., Warren, H.R., Wang, Y.-M.: 2004, *Astrophys. J.* **616**, 1224.
Sturrock, P.A.: 1966, *Nature* **211**, 695.
Urpo, S., Teräsranta, H., Krüger, A., Hildebrandt, J., Ruždjak, V.: 1989, *Astron. Nachr.* **310**(6), 423.
Zhitnik, I.A., Bugaenko, O.I., Ignat'ev, A.P., Krutov, V.V., Kuzin, S.V., Mitrofanov, A.V., Oparin, S.N., Pertsov, A.A., Slemzin, V.A., Stepanov, A.I., Urnov, A.M.: 2003, MNRAS, **338**, 67.